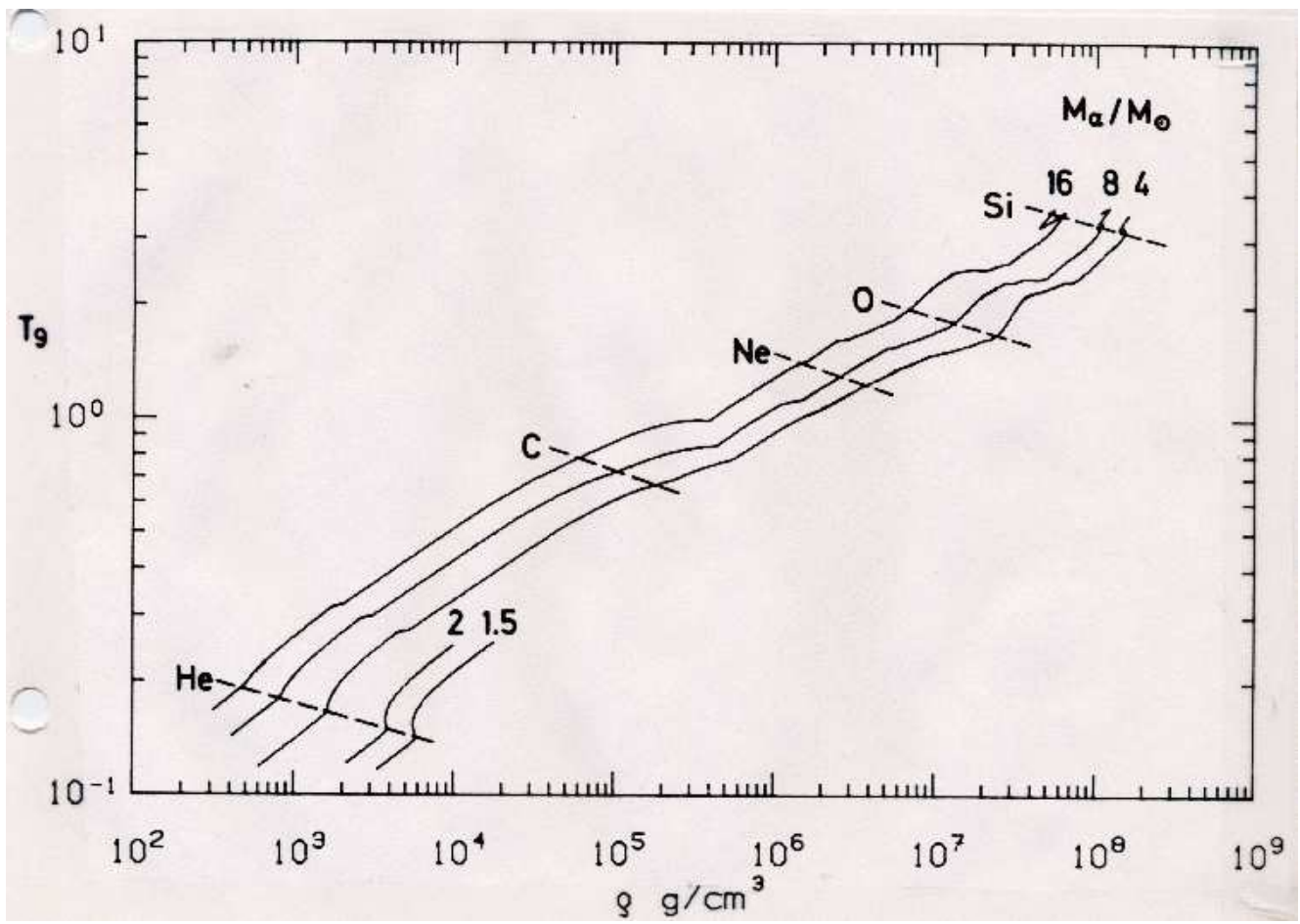


## The Carbon Flash

Because of the strong electrostatic repulsion of carbon and oxygen, and because of the plasma cooling processes that take place in a degenerate carbon-oxygen core, it is extremely difficult to fuse carbon. As long as the core remains under the Chandrasekhar limit, degeneracy pressure can support the star, and nuclear reactions will not occur. Stars with initial masses  $\mathcal{M} \lesssim 7\mathcal{M}_\odot$ , will probably stay under this limit, and thus their nuclear evolution will end with carbon.

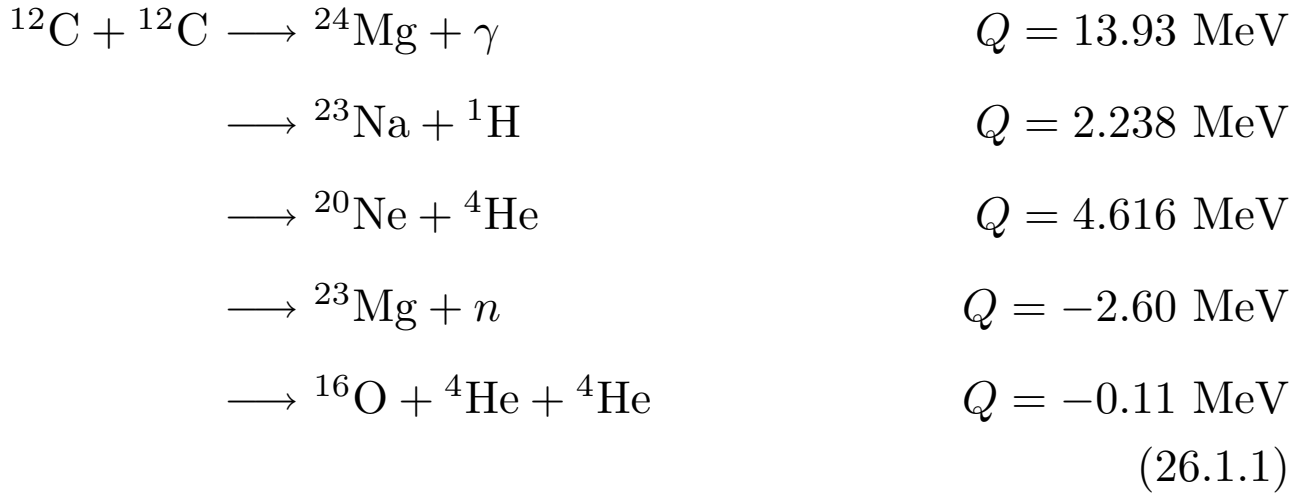
If helium burning creates a core that is greater than the Chandrasekhar mass, the core will collapse, and carbon fusing will occur. In objects with initial masses  $8 \lesssim \mathcal{M} \lesssim 10\mathcal{M}_\odot$ , this fusion will occur under extremely degenerate conditions; the result is an explosive carbon flash. (The timescale for this burning will be milliseconds!) A *deflagration front* will probably develop, in which the shock wave itself does not ignite carbon, but instead, carbon is fused by the energy transported behind the shock front. (The alternative to this is a *detonation front*, where the shock itself ignites the fuel.) Either way, the star does not have time to adjust to the energy input, and the energy released ( $Q \sim 2.5 \times 10^{17}$  ergs  $\text{gm}^{-1}$ ) is enough to disrupt the entire core.



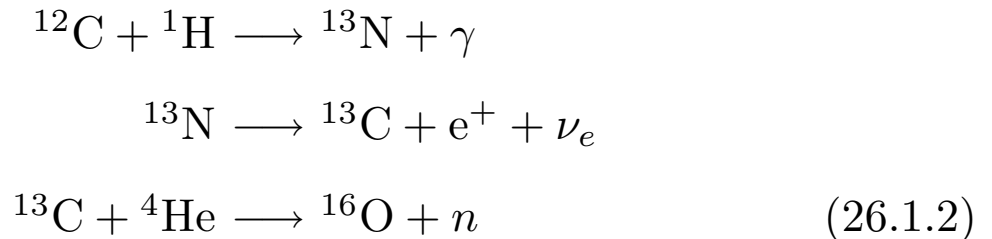
Core evolution for high mass stars after helium-core burning.

## Carbon Burning

In higher mass stars, the core temperatures are sufficient to fuse carbon under non-degenerate conditions. When this happens a  $^{12}\text{C}$  nucleus fuses with another  $^{12}\text{C}$  nucleus to form a compound excited state of  $^{24}\text{Mg}$  through one of many resonances that exist. The  $^{24}\text{Mg}$  then decays through one of many channels:



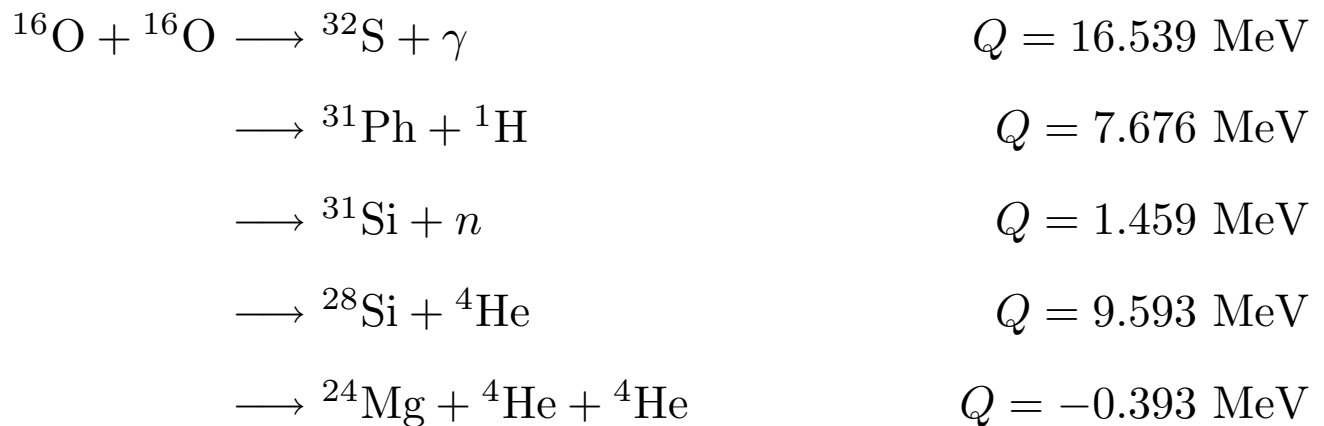
with the electromagnetic and 3-body channels having the lowest probabilities, and the neutron reaction requiring the highest particle energy. Thus, to first order,  $^{12}\text{C}$  fuses to  $^{23}\text{Na}$  and  $^{20}\text{Ne}$ . However the protons and  $\alpha$  particles quickly fuse as well, with many possible combinations. The most likely are



(This last reaction is important, since it creates a free neutron, which can be used to synthesize heavier elements.) In addition, the  $\alpha$  particles may also interact with  $^{12}\text{C}$ ,  $^{16}\text{O}$ ,  $^{20}\text{Ne}$ , and  $^{24}\text{Mg}$ . The net result is that even though  $^{12}\text{C}$  fusion itself does not produce a

large amount of energy, the additional reactions raise the amount of energy liberated to  $\sim 13$  MeV per reaction.

Although carbon and oxygen are roughly in equal abundance in the core, reactions between  $^{12}\text{C}$  and  $^{16}\text{O}$  are not important, due to the additional coulomb barrier. (By the time the temperature is high enough to fuse carbon with oxygen, all the carbon is gone.) Thus, the next series of reactions that take place are resonance reactions involving two oxygen nuclei:



As in the case of carbon burning, the protons, neutrons, and  $\alpha$  particles produced by this reaction can interact with a host of other nuclei, and thus a large reaction network must be analyzed. The primary product of oxygen burning is  $^{28}\text{Si}$ , but a wide range of elements are produced.

## Photodisintegration

At temperature of  $T \sim 10^9$  K (which is typical of carbon and oxygen burning), nuclei can become disassociated by the thermal photon bath. This is the exact analog of photo-ionization of electrons (except, of course, that the temperatures are very much higher).

Photodisintegration rates can be calculated in the exact same manner as photoionization rates. Consider the reaction



In thermodynamic equilibrium, the photodisintegration rate,  $\lambda_\gamma$ , must be related to the reaction rate  $\lambda_{XY}$  by

$$N_Z \lambda_\gamma = N_X N_Y \lambda_{XY}$$

and the ratios of the species  $X$ ,  $Y$ , and  $Z$  must be given by the Saha equation

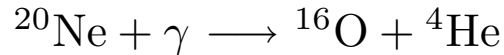
$$\left( \frac{N_X N_Y}{N_Z} \right) = \frac{G_X G_Y}{G_Z} \left( \frac{2\pi\mu kT}{h^2} \right)^{3/2} e^{-Q/kT} \quad (26.2.2)$$

where the  $G$  values are the nuclear partition functions,  $\mu$  is the reduced mass of the system, and  $Q$  is the binding energy. Thus we have

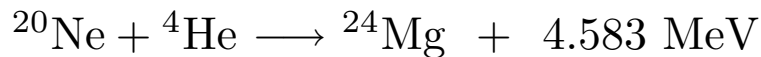
$$\begin{aligned} \lambda_\gamma &= \frac{G_X G_Y}{G_Z} \left( \frac{2\pi\mu kT}{h^2} \right)^{3/2} e^{-Q/kT} \lambda_{XY} \\ &= 5.943 \times 10^{33} \frac{G_X G_Y}{G_Z} (AT_9)^{3/2} \exp\left(-\frac{11.605 Q}{T_9}\right) \lambda_{XY} \end{aligned} \quad (26.2.3)$$

where  $A$  is the reduced atomic weight, and  $Q$  is in MeV.

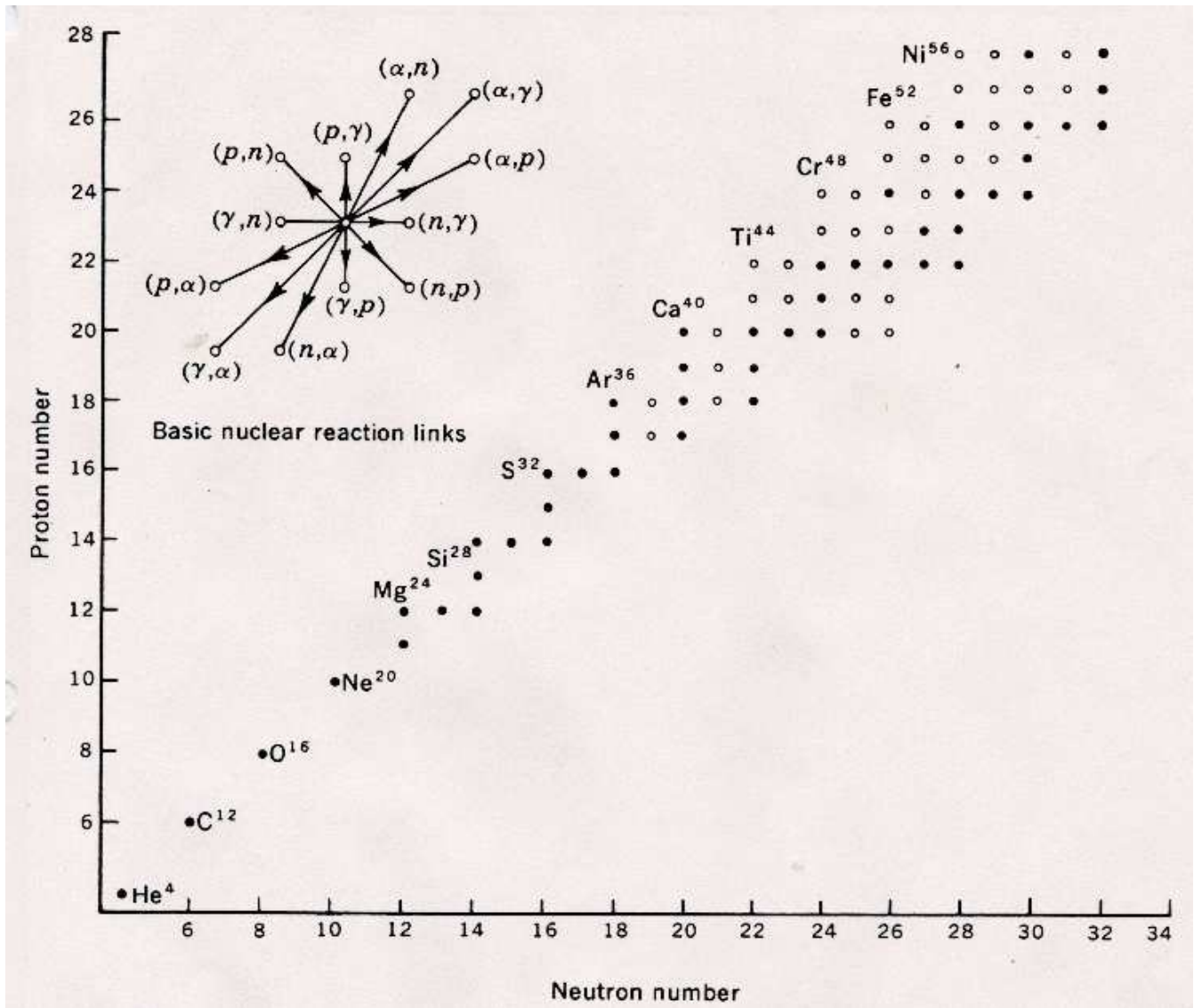
During carbon-oxygen burning,  $^{13}\text{N}$  and  $^{20}\text{Ne}$  are the principal victims of photodisintegration. At temperature  $T_9 > 0.75$ , the photodisintegration of  $^{13}\text{N}$  is faster than its beta decay, and thus the concentration of  $^{13}\text{C}$  is sharply reduced. Similarly, at  $T_9 > 1.3$ , the photodisintegration of  $^{20}\text{Ne}$  into oxygen and helium is greater than its creation rate from oxygen and helium. Thus



Interestingly, the  $\alpha$  particle produced by this reaction is now free to fuse with a different  $^{20}\text{Ne}$  nucleus, giving



Thus,  $^{20}\text{Ne}$  only exists for a short time in the star: it is made during carbon burning at  $T_9 \sim 0.7$  and destroyed during carbon burning at  $T_9 \sim 1.3$ .

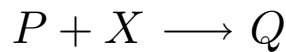


The nuclei which participate in the reaction network during silicon burning. The solid dots designate stable nuclei (*i.e.*, observables); the open dots denote unstable nuclei. (See Truran, Cameron, & Gilbert 1966, *Can. J. Phys.*, **44**, 576.)

## Photodisintegration Rearrangement

Since carbon and oxygen burning generate products such as  $^{24}\text{Mg}$ ,  $^{28}\text{Si}$ , and  $^{32}\text{Si}$ , it is tempting to consider the next step where these elements get fused. However, the coulomb barrier for these species is so large, that photodisintegration will occur before their fusion temperature is reached. Instead, further elemental fusion occurs via protons, neutrons, and  $\alpha$  particles that have been photodisintegrated from nuclei with small binding energies.

Now consider the reaction specified in (26.2.1). If the photon bath is high, this reaction will attempt to come to equilibrium, and establish the abundance ratios given by the nuclear Saha equation (26.2.2). However, once removed from nucleus  $Z$ , particle  $X$  may also fuse with a different nucleus,  $P$ , *i.e.*,



and nucleus  $Q$  may have a binding energy high enough to resist photodisintegration. Thus the abundance of element  $Q$  may be increased, and that of element  $Z$  may be decreased by *photodisintegration rearrangement*. This may, or may not create nuclear energy (since many of the reactions involve energy losses from neutrinos), but it will certainly relocate nucleons into those nuclei that are the most tightly bound.

The results of photodisintegration rearrangement depend on the exact temperature and timescale of the burning process. Many of the species formed during the process will be radioactive, and their positron-decays will reduce the total proton-to-neutron ratio. (Again, the importance of these decays will depend on the timescale of the burning through their temperature dependence.)



The computation of nucleosynthesis during photodisintegration requires following a series of long differential equations containing all the reactions that can create or nuclei, *i.e.*,

$$\begin{aligned}
\frac{dN(A, Z)}{dt} = & -\lambda_\gamma(A, Z)N(A, Z) + \lambda_{\gamma,n}(A+1, Z)N(A+1, Z) \\
& + \lambda_{\gamma,p}(A+1, Z+1)N(A+1, Z+1) \\
& + \lambda_{\gamma,\alpha}(A+4, Z+2)N(A+4, Z+2) \\
& - N(A, Z)N(n) \lambda_n(A, Z) \\
& - N(A, Z)N(p) \lambda_p(A, Z) \\
& - N(A, Z)N(\alpha) \lambda_\alpha(A, Z) \\
& + N(A-1, Z)N(n) \lambda_n(A-1, Z) \\
& + N(A-1, Z-1)N(p) \lambda_p(A-1, Z-1) \\
& + N(A-4, Z-2)N(\alpha) \lambda_\alpha(A-4, Z-2) \\
& - \lambda_\beta(A, Z)N(A, Z) \\
& + \lambda_\beta(A, Z-1)N(A, Z-1) + \dots
\end{aligned}$$

(Note that the above equation does not even include reactions such as  $X + p \longrightarrow Y + n$ ,  $X + n \longrightarrow Y + \alpha$ , *etc.*) Much of the work in setting up the network of equations is in deciding which reactions are important, and which can be neglected.)

At oxygen burning temperatures, nuclei such as  $^{32}\text{S}$ ,  $^{31}\text{P}$ , and  $^{30}\text{Si}$  are all destroyed in favor of  $^{28}\text{Si}$ , which is the most tightly bound nucleus in the intermediate mass range. Once the temperature becomes high enough to photodisintegrate  $^{28}\text{Si}$  ( $T_9 \gtrsim 3$ ), a host of  $(\alpha, \gamma)$ ,  $(p, \gamma)$ ,  $(n, \gamma)$  reactions (and their inverses) begin simultaneously. This is the *Silicon Burning* phase. Some of the fastest

reactions run to equilibrium, but most reactions will not reach this stage. Thus, the results of silicon burning depend on how far towards completion the reactions run. During this time, there is also a slow leakage of nuclei from the intermediate-mass region to the iron group (which are the most tightly bound nuclei).

As silicon burning nears completion, the nuclei come closer and closer to establishing nuclear statistical equilibrium. In this case, the nuclear Saha equation defines the abundance of each species. This has a very simple form. Consider that, from the Saha equation, the abundance ratio of species  $A-1, Z$  to  $A, Z$  is

$$\begin{aligned} \frac{N(A-1, Z)N_n}{N(A, Z)} &= \frac{G_n G(A-1, Z)}{G(A, Z)} \left( \frac{2\pi\mu kT}{h^2} \right)^{3/2} \exp\left(-\frac{Q_1}{kT}\right) \\ &= \frac{2G(A-1, Z)}{G(A, Z)} \Theta \left( \frac{A-1}{A} \right)^{3/2} \exp\left(-\frac{Q_1}{kT}\right) \end{aligned}$$

where  $G$  is the nuclear partition function (2 for the neutron),  $Q_1$  is the binding energy of  $A-1, Z$ , and  $\Theta = (2\pi m_a kT/h^2)^{3/2}$ . Similarly, we can write an expression for the ratio of species  $A-2, Z-1$  in terms of  $A-1, Z$

$$\frac{N(A-2, Z-1)N_p}{N(A-1, Z)} = \frac{2G(A-2, Z-1)}{G(A-1, Z)} \Theta \left( \frac{A-2}{A-1} \right)^{3/2} \exp\left(-\frac{Q_2}{kT}\right)$$

where  $Q_2$  is the binding energy of this new species. If you multiply these two equations, then you obtain a relation between  $A, Z$ , and  $A-2, Z-1$

$$\begin{aligned} \frac{N(A-2, Z-1)N_n N_p}{N(A, Z)} &= \frac{2^2 G(A-2, Z-1)}{G(A, Z)} \Theta^2 \left( \frac{A-2}{A} \right)^{3/2} \\ &\quad \exp\left(-\frac{Q_1 + Q_2}{kT}\right) \end{aligned} \tag{26.2.4}$$

This progression can be taken all the way to  $Z = A = 1$ , with the result

$$N(A, Z) = \frac{G(A, Z)}{2^A} A^{3/2} N_p^Z N_n^{A-Z} \Theta^{1-A} \exp\left(-\frac{Q}{kT}\right) \quad (26.2.5)$$

where

$$Q = (Zm_H + (A - Z)M_n - M(A, Z)) c^2 \quad (26.2.6)$$

is the binding energy of the nucleus  $A, Z$ . Note the resultant abundances are a function only of the temperature, the binding energy of the species, and the number density of protons and neutrons. Note also that the latter two quantities are constrained. Since the density of the star is known, we have from (5.1.1)

$$N_A \rho = N_p + N_n + \sum N_i A_i \quad (26.2.7)$$

Moreover, if we parameterize the system with the quantity  $\bar{Z}/\bar{N}$ , *i.e.*, the average proton to neutron ratio, then

$$\frac{\bar{Z}}{\bar{N}} = \frac{\sum Z N(A, Z) + N_p}{\sum (A - Z) N(A, Z) + N_n} \quad (26.2.8)$$

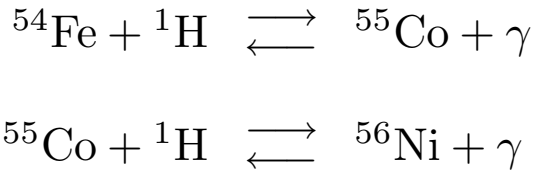
Thus (26.2.5), (26.2.7), and (26.2.8) form a set of three equations with three unknowns, and  $\rho$ ,  $T$ , and  $\bar{Z}/\bar{N}$  described the entire set of nuclear abundances.

Unfortunately, the analysis above is not completely accurate, since it fails to account for reactions that involve the weak nuclear force, *i.e.*, beta decays. Since the neutrinos from these decays leave the star, there is no inverse reaction associated with beta-decays, and no equilibrium condition. To first order, however, the effect of beta-decays can be modeled through their impact on  $\bar{Z}/\bar{N}$ . Thus,

$$\left(\frac{\bar{Z}}{\bar{N}}\right)_{t+\Delta t} \approx \left(\frac{\bar{Z}}{\bar{N}}\right)_t + \Delta t \frac{\partial}{\partial t} \left(\frac{\bar{Z}}{\bar{N}}\right)_t \quad (26.2.9)$$

The computation of beta-decay rates is a bit trickier than normal, since many of the decays come from excited nuclear states, and the high densities increase the probability of electron captures by a factor of  $\sim 100$  over terrestrial conditions. However, these reactions are important, in that a small change in  $\bar{Z}/\bar{N}$  greatly affects the composition of the iron group. Clearly, the faster the reactions proceed, the less time there is for beta-decay, and the closer  $\bar{Z}/\bar{N}$  will be to 1.

The question of beta-decays and the value of  $\bar{Z}/\bar{N}$  has important consequences for supernova calculations and for cosmic abundance determinations. For example, consider silicon burning, where  $^{28}\text{Si}$  is converted to iron peak elements. Let's examine the case where the two dominant resultant species are  $^{54}\text{Fe}$  and  $^{56}\text{Ni}$ . These nuclei are in statistical equilibrium via the reactions



If  $^{28}\text{Si}$  burns to  $^{56}\text{Ni}$ , then the reaction is exothermic with an net energy release of 10.9 MeV and the star can continue burning; on the other hand, if the result is  $^{54}\text{Fe} + 2p$ , then  $-1.3$  MeV is lost in the reaction, and the star will collapse. From (26.2.4), the ratio between  $^{54}\text{Fe}$  and  $^{56}\text{Ni}$  is

$$\frac{N(^{54}\text{Fe})}{N(^{56}\text{Ni})} N_p^2 = 2^2 \frac{G(^{54}\text{Fe})}{G(^{56}\text{Ni})} \left(\frac{54}{56}\right)^{\frac{3}{2}} \Theta^2 \exp \left\{ -\frac{Q(^{55}\text{Co}) + Q(^{56}\text{Ni})}{kT} \right\}$$

The ratios of the partition functions for these two species is  $\sim 1$ , so plugging in the numbers yields

$$\frac{N(^{54}\text{Fe})}{N(^{56}\text{Ni})} N_p^2 = T_9^3 10^{68.13 - 62.09/T_9} \quad (26.2.10)$$

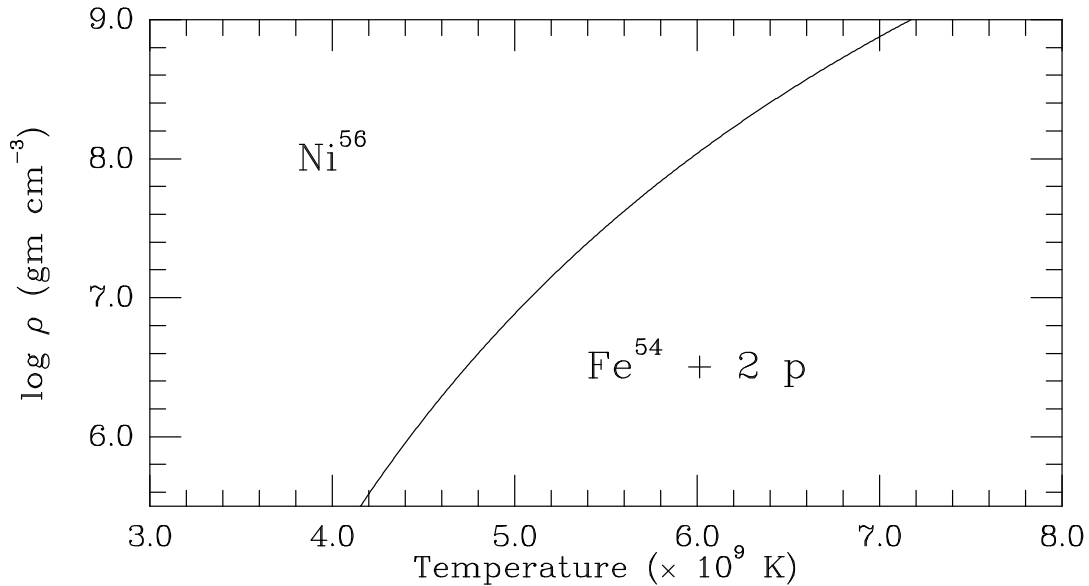
We can now substitute for  $N_p$  using (26.2.8); if  $\bar{Z}/\bar{N} = 1$

$$\frac{\bar{Z}}{\bar{N}} = 1 \approx \frac{26N(^{54}\text{Fe}) + 28N(^{56}\text{Ni}) + N_p}{28N(^{54}\text{Fe}) + 28N(^{56}\text{Ni})} \implies N_p \approx 2N(^{54}\text{Fe})$$

Substituting this in (26.2.10) gives

$$\frac{N(^{54}\text{Fe})^3}{N(^{56}\text{Ni})} = \frac{N_A^2 X(^{54}\text{Fe})^3 A(^{56}\text{Ni})}{X(^{56}\text{Ni}) A(^{54}\text{Fe})^3} \rho^2 = T_9^3 10^{67.53 - 62.09/T_9}$$

Thus, for  $X(^{54}\text{Fe}) = X(^{56}\text{Ni})$ ,  $\rho^2 \approx T_9^3 10^{24.09 - 62.09/T_9}$



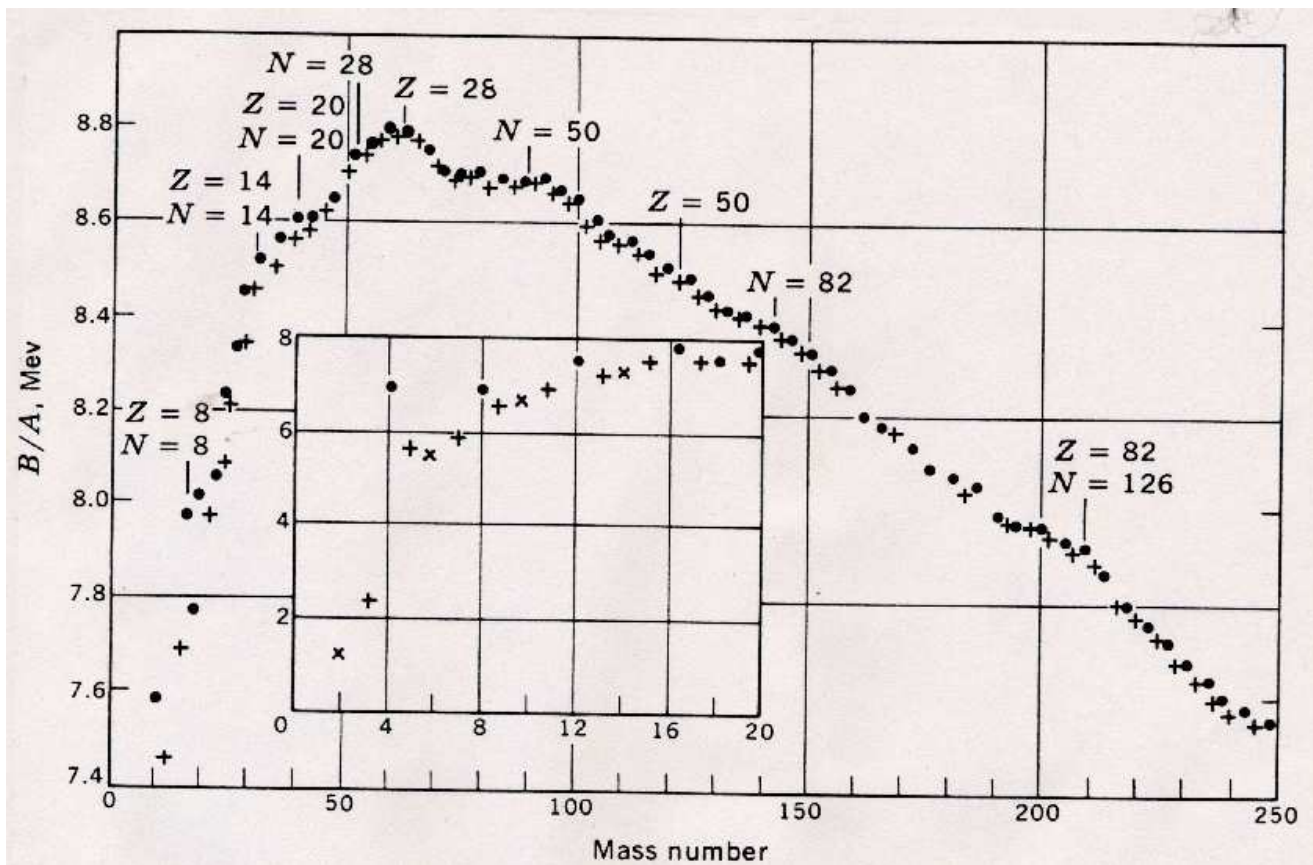
The graph for  $\bar{Z}/\bar{N} = 1$  shows that at low temperatures,  $^{28}\text{Si}$  will fuse to  $^{56}\text{Ni}$  (which then beta-decays to  $^{56}\text{Fe}$ ); this reaction provides energy to supports the star. However, if  $^{28}\text{Si}$  burns at a high temperature,  $^{54}\text{Fe}$  will result, and the star will collapse.

This process of nucleosynthesis is call the *e-process*, for equilibrium process.

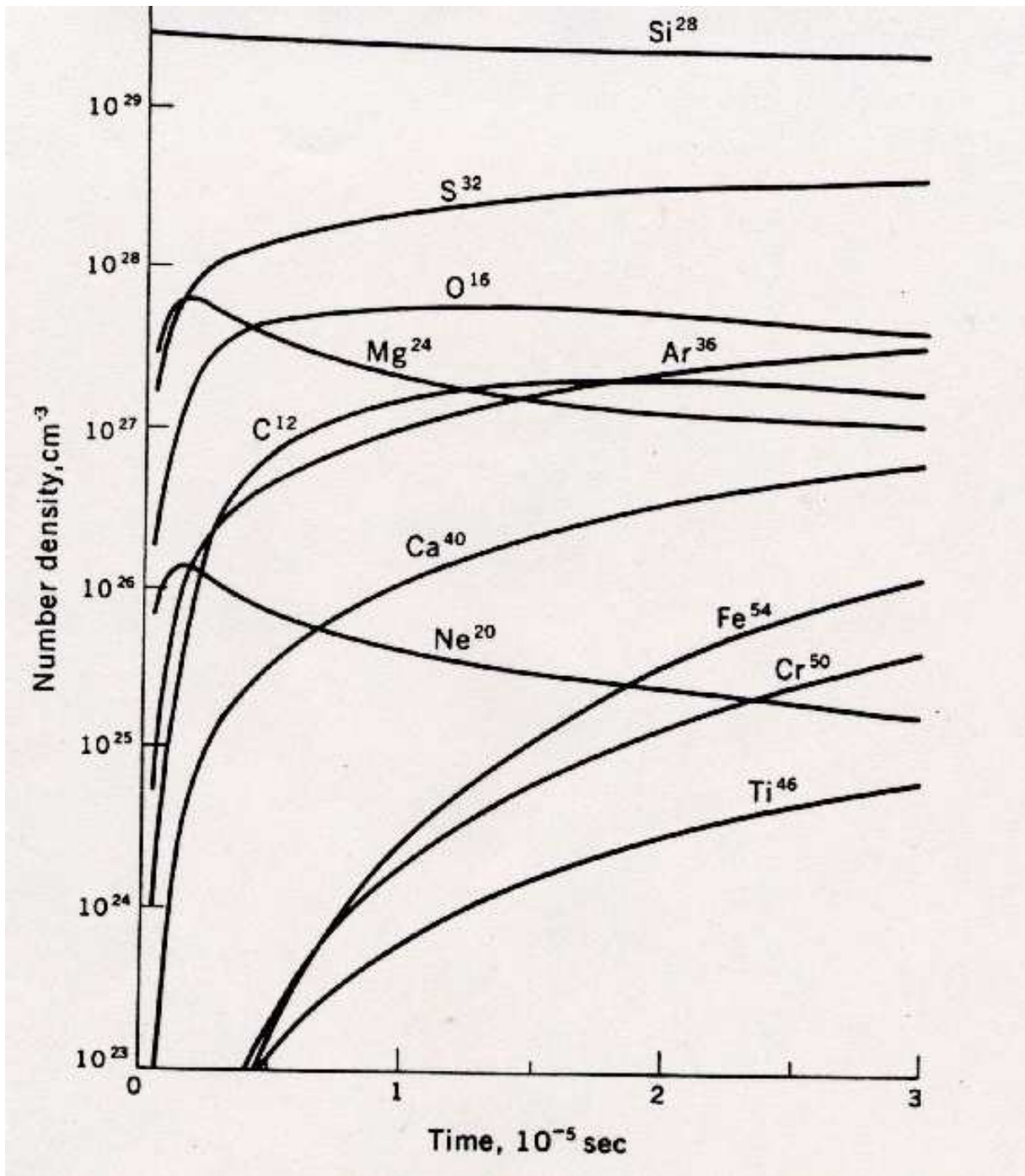
In general, the peak iron element will have approximately the same proton to neutron ratio as given by  $\bar{Z}/\bar{N}$ . Thus,

$$\frac{\bar{Z}}{\bar{N}} \approx \frac{26}{28} \implies {}^{54}\text{Fe} \quad \text{while}$$
$$\frac{\bar{Z}}{\bar{N}} \approx \frac{26}{30} \implies {}^{56}\text{Fe}$$

In nature, the most abundant isotope in the iron group is  ${}^{56}\text{Fe}$ , with 26 protons and 30 neutrons. This suggests that the e-process usually either occurs very rapidly at low temperatures, so that  ${}^{56}\text{Fe}$  is produced via the decay of  ${}^{56}\text{Ni}$ , or proceeds very slowly so that beta-decays make  $\bar{Z}/\bar{N} \approx 0.87$ .

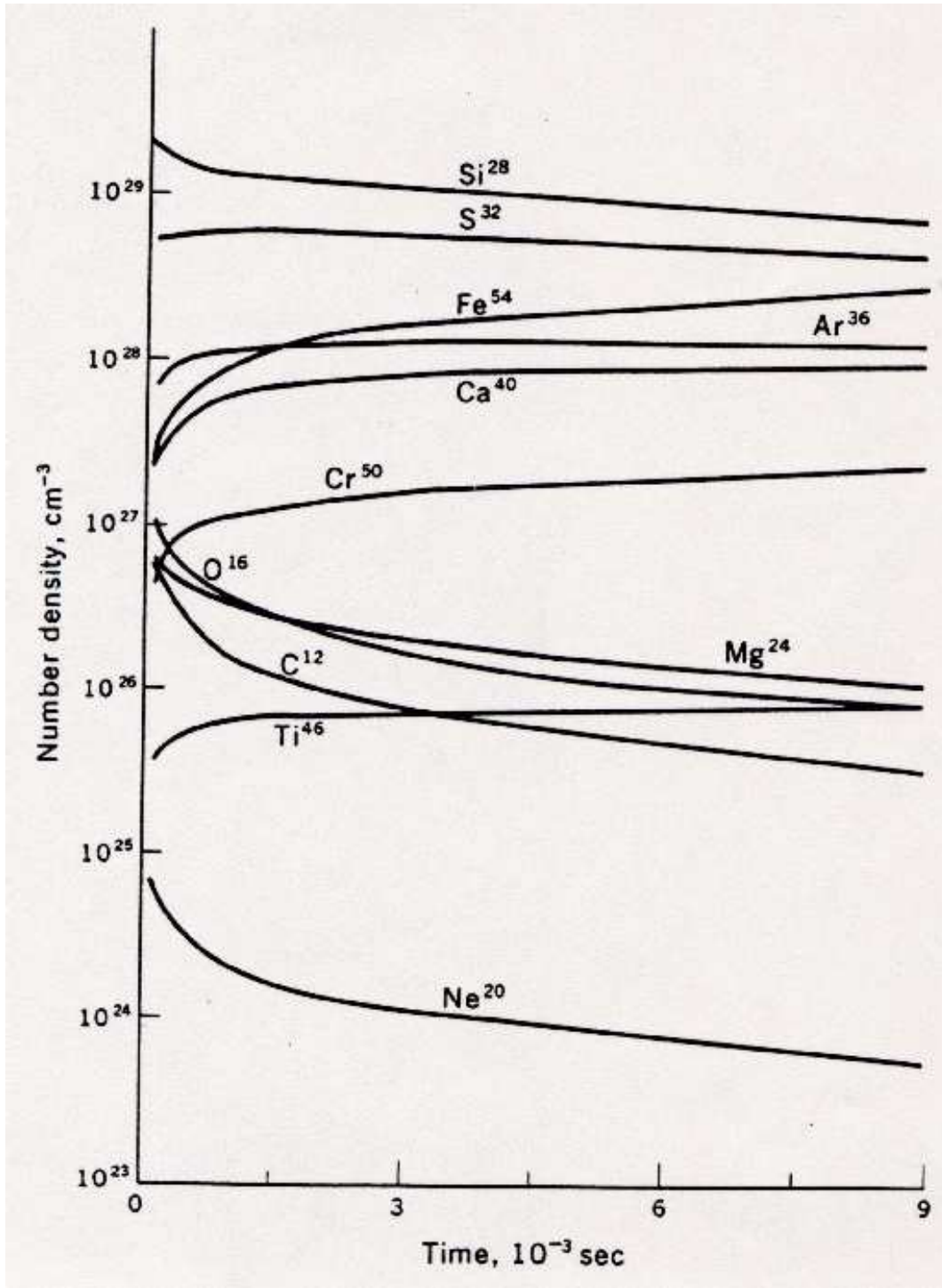


The binding energy per nucleon of the most stable nucleus of each atomic weight. The solid circles represent nuclei with even numbers of protons and an even number of neutrons, while the crosses show odd- $A$  nuclei.

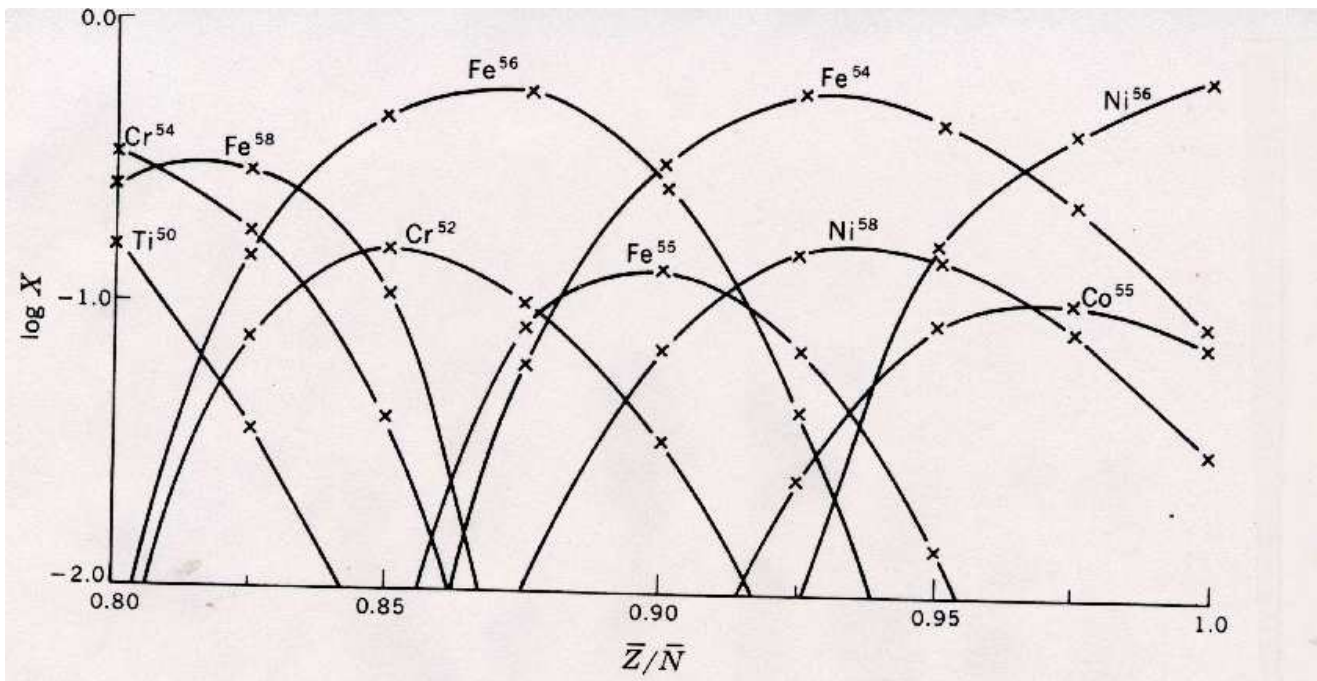


The early phase of nuclear rearrangement of initially pure  $^{28}\text{Si}$  at  $T = 5 \times 10^9$  K and  $\rho = 1.3 \times 10^7$  g cm $^{-3}$ . The abundances grow very rapidly at first, as the liberated alpha particles are consumed in the rapid flow towards the iron group.

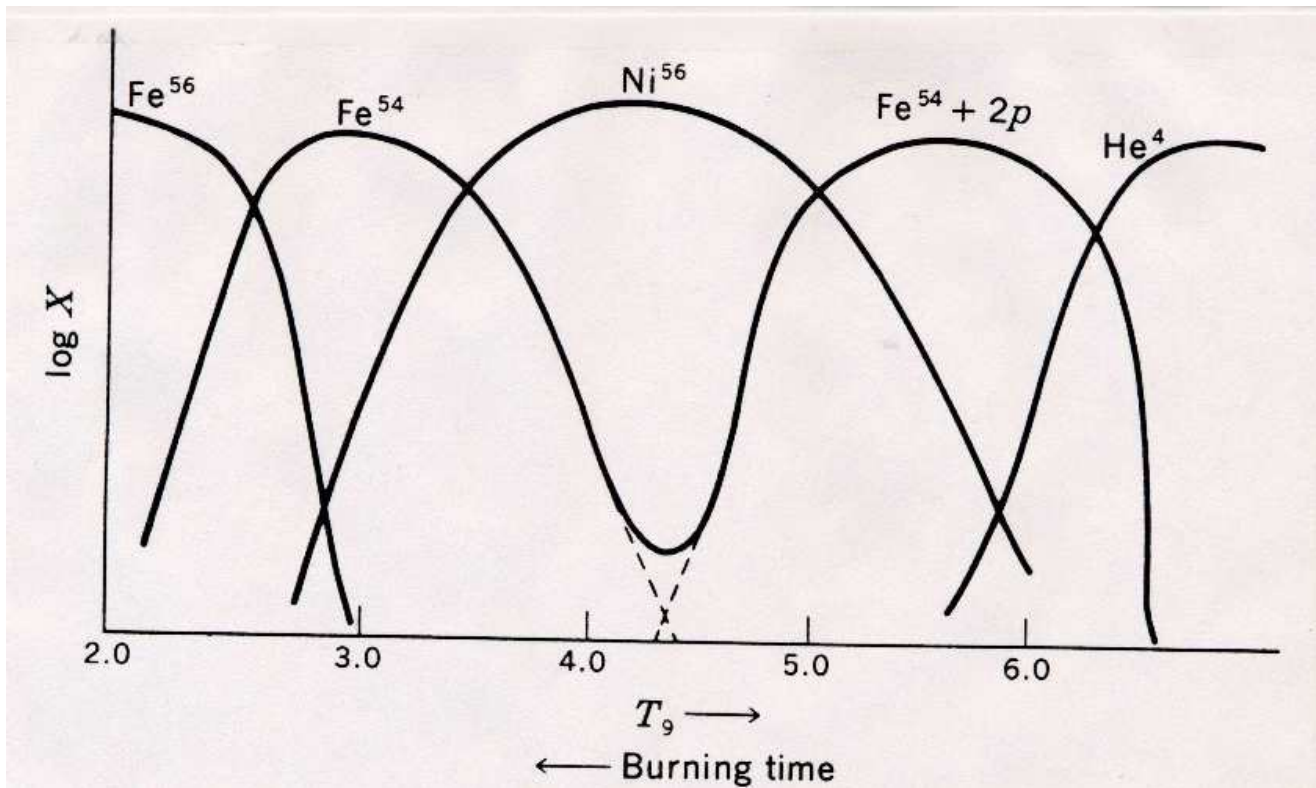




Number densities of key nuclei during silicon burning at  $T = 5 \times 10^9$  K at later times. The densities of free protons and neutrons have become nearly quasistatic as a result of the near equilibrium between their rate of capture and their photoejection into the nuclei heavier than  $^{28}\text{Si}$ . All the heavier nuclei have approached a quasi-equilibrium with  $^{28}\text{Si}$  and the pool of free nucleons, so their abundances also change very little.



Mass fractions of the most abundant nuclear species in nuclear statistical equilibrium at  $T = 4 \times 10^9$  K and  $\rho = 10^6$  g cm $^{-3}$ . As the value of  $\bar{Z}/\bar{N}$  is reduced, the equilibrium shifts to more neutron-rich nuclei (Clifford & Taylor 1965, *Mem. Roy. Astron. Soc.*, **69**, 21.)



A schematic of the principal nuclei that result from the burning of silicon. For  $T > 4 \times 10^9$  K, the burning is so fast that  $\bar{Z}/\bar{N} = 1$  throughout the burning. The time required for the burning increases greatly as the temperature is decreased; this results in lower values for  $\bar{Z}/\bar{N}$ . Near  $T \sim 3 \times 10^9$  K, the neutron-rich nucleus  $^{54}\text{Fe}$  has sufficient time to appear; at even lower temperatures the beta decays drive the equilibrium to  $^{56}\text{Fe}$ .